JOURNAL OF AIRCRAFT
Vol. 31, No. 2, March–April 1994

Forebody Vortex Control for Wing Rock Suppression

T. T. Ng*
University of Toledo, Toledo, Ohio 43606
and
C. J. Suarez,† B. R. Kramer,‡ L. Y. Ong,§ B. Ayers,¶ and G. N. Malcolm**
Eidetics International, Inc., Torrance, California 90505

Static and free-to-roll tests were conducted in a water tunnel and a wind tunnel with a configuration that consisted of a highly slender forebody and 78-deg-sweep delta wings. The mechanisms governing the wing rock of this configuration are the interactions between the forebody and the wing vortices. Means of suppressing wing rock by controlling the forebody vortices using small blowing jets were explored. Steady blowing tangentially aft from leeward nozzles near the forebody tips was found to be capable of suppressing wing rock. The wing rock motion was attenuated at low blowing rates and eliminated at high blowing rates. At high blowing rates, however, significant vortex asymmetries were also induced. On the other hand, alternating pulsed blowing on the left and right sides of the forebody was demonstrated to potentially be an effective means of suppressing wing rock without creating, on a time-average basis, large flow asymmetries.

Nomenclature

A_{ref} = reference wing area, equal to 552 cm² for the water-tunnel model and 2208 cm² for the wind-tunnel model
b = wing span
C_n = body axis yawing moment coefficient, $yM/q_\infty A_{ref}l$
C_p = pressure coefficient
C_Y = body axis side force coefficient
C_μ = momentum coefficient of blowing, $mjV_j/q_\infty A_{ref}$
c = wing chord
f = wing rock frequency
k = reduced frequency, $\pi fb/U_\infty$
L = reference length, total length of the model
LF = left forebody vortex, from a pilot's viewpoint
LW = left wing vortex, from a pilot's viewpoint
m_j = mass flow rate of the blowing jet
q_∞ = freestream dynamic pressure
RF = right forebody vortex
RW = right wing vortex
t^* = convective time, tU_∞/L
U_∞ = freestream velocity
V_j = average exit velocity of the blowing jet
yM = yawing moment
α = angle of attack
β = angle of sideslip
$\Delta\phi$ = roll or wing rock amplitude (peak-to-peak value)
Φ = angle from the windward meridian
ϕ = model roll angle
ϕ^* = normalized roll angle, $2\phi/\Delta\phi$

I. Introduction

MODERN fighter aircraft are operating in a flight regime that requires maximum maneuverability and controllability to be effective in the combat arena. One of the limitations to combat effectiveness for all fighter aircraft is the phenomenon of wing rock—a moderate to high angle-of-attack dynamic motion manifested primarily in a limit-cycle oscillation in roll with, in some cases, a coupled oscillation in yaw. Generally, the onset of wing rock is attributed to a loss of stability in the lateral/directional mode and can be caused by a number of different aerodynamic phenomena.[1,2]

At high angles of attack, the vortices emanating from the forebody of an aircraft can be very strong. Studies[3,4] have shown that these vortices control wing rock in this flight regime. While this form of wing rock is undoubtedly configuration dependent, it is generally believed that interactions between asymmetric forebody vortices with the other surfaces on the aircraft at sideslip conditions are the main mechanism that drives the motions. Once the rocking motion is initiated, dynamic flow phenomena over the moderately swept wings and highly swept leading-edge extensions (LEXs) may also contribute to the building-up of wing rock.

Attempts have been made in recent years on specific aircraft configurations[5,6] using a variety of both controls-oriented and aerodynamic fixes to cure wing-rock problems. For instance, wind-tunnel and drop-test results[7] indicate that the X-29A aircraft exhibits negative roll damping at α above about 18 deg. A conventional roll damper can eliminate wing rock below about 35-deg angle of attack, but is ineffective at higher angles of attack where wing rock is induced by forebody vortices. The loss of effectiveness of a conventional roll damper at high α is likely to be common for many modern fighters, and can severely limit aircraft capabilities in a rather critical flight regime. Even if the conventional control surfaces, such as the aileron and rudder, can effectively control wing rock, the level of control power remaining for maneuvering may be insufficient to meet the high angle-of-attack maneuverability requirements. An alternative source for roll stability control would help solve this problem.

The powerful forebody vortices are one of the main causes of aircraft instabilities at high angles of attack. Directly controlling these vortices is an effective means of suppressing the instabilities at this flight regime. The use of symmetrically deployed forebody strakes has been shown to be effective in forcing naturally occurring asymmetric vortices at high angles of attack to be symmetric. The use of asymmetrically deployed forebody strakes has been investigated recently for possible application to controlling the yawing moment.[8,9] Rotatable nose-tip devices are also found to be effective in controlling

Received Sept. 24, 1992; revision received Dec. 23, 1992; accepted for publication Dec. 28, 1992.

*Associate Professor, Department of Mechanical Engineering. Member AIAA.
†Staff Engineer, 3415 Lomita Blvd. Member AIAA.
‡Senior Engineer, 3415 Lomita Blvd. Member AIAA.
§Engineer, Singapore Aerospace. Member AIAA.
¶Technician, 3415 Lomita Blvd.
**Vice President, Aeronautics Division, 3415 Lomita Blvd. Associate Fellow AIAA.

the forebody flow.[10-12] Various forebody-blowing techniques have also been investigated[9,13-15] and were found to be highly effective in controlling the vortex orientation.

Up to now, most of the studies on forebody vortex control have been concentrated on directional control. In situations where wing rock is controlled by the forebody vortices, forebody vortex control should also have an impact on the wing rock motion. The main goals of the present study are to determine if controlling the vortex asymmetries can induce sufficiently strong roll damping so that wing rock can be suppressed, and to identify effective means of control. Experiments were performed on a highly slender forebody-wing model. The model possesses characteristics that may be considered as similar to certain aircraft forebody/LEX and missile forebody-canard combinations. The specific objectives are 1) to investigate possible causes of wing rock on a highly-slender forebody-wing configuration; 2) to study the vortex flows over the wing and forebody during wing rock; and 3) to explore the effectiveness of forebody vortex control in the form of blowing jets operating near the forebody tip in controlling wing rock of the configuration.

Wind-tunnel experiments were performed to obtain quantitative information needed to achieve the above objectives. In addition, water-tunnel experiments were performed to provide detailed flow visualizations. The effects of Reynolds number and model inertia could also be investigated by comparing results from the two sets of experiments.

II. Experimental Setup

The wind-tunnel model can be seen in Fig. 1. The forebody of the model has a length-to-base-diameter ratio of 6, and was circular in cross section with a projected side-profile as shown, which resulted in a nominal apex angle of about 18.5 deg. The wings were sharp-edge delta wings with a 78-deg sweep. Two low-friction bearings allow the model to rotate "freely" around its longitudinal axis. A rotational transducer is used to measure the roll angle history. An electromagnetic brake was used to release the model from a static position. Two basic configurations were tested: 1) tail-on and 2) tail-off. Each configuration was statically balanced in roll by means of lead weights bolted internally to the model.

The forebody of the model is provided with three rings of static pressure ports. Dynamic pressure transducers, located on each wing at 93 and 118.4 cm from the tip, provided time-resolved wing pressure data. A six-component sting balance was used to acquire force data.

The blowing ports are located at fuselage station (FS) 3.2 cm, and $\Phi = \pm 150$-deg radially from the windward meridian. The blowing was controlled by two fast-acting solenoid valves. The total pressure and temperature in a chamber very close to each of the nozzle exits were measured to determine the mass flow rate and the blowing coefficient. The interference of the blowing lines with the wing rock motion was minimized by leaving a large service loop behind the model.

The wind-tunnel experiments were conducted in the NASA Ames 7- × 10-ft wind tunnel. It is a closed-throat, single return atmospheric tunnel with about 10% air exchange, accomplished by means of a ventilating tower. The experiments were conducted at a dynamic pressure ranging from 718 Pa (19.8 m/s) to 1436 Pa (39.6 m/s), corresponding to Reynolds numbers from 280,000 to 400,000 based on the forebody base diameter.

The water-tunnel model was half the scale of the wind-tunnel model. Tests were conducted with no vertical tail, with tail A (similar to the wind-tunnel model tail), and with tail B (about two times the area of tail A). Blowing ports were located near the tip of the forebody, 1.9 cm from the apex, with the 0.76-mm-diam nozzles pointing directly aft along the $\Phi = \pm 150$-deg meridians. The blowing fluid was supplied by a pressurized cannister and metered by a rotometer. Blowing on the left and right sides were turned on or off by fast-acting solenoid valves. For the pulsed blowing, the nominal blowing rate was set initially with the valve opened.

Two bearings spanned on a mounting bracket along the centerline of the fuselage allows a single degree-of-freedom, "free-to-roll" motion about the body axis. The model was balanced so that its c.g. aligned closely with the roll axis. The roll angle was indicated by markings at the tail end of the model and a pointer on the support sting. Close-up video recordings of the tail end during wing rock allowed the roll angle history to be obtained in subsequent data processing.

The water-tunnel experiments were conducted in a continuous horizontal flow tunnel with a test section 0.71 m high × 0.61 m wide × 1.83 m long. Most of the tests were conducted at a flow speed of about 0.19 m/s, corresponding to Reynolds number of 10,200, based on the body diameter. A pressurized dye-injection system was used for flow visuali-

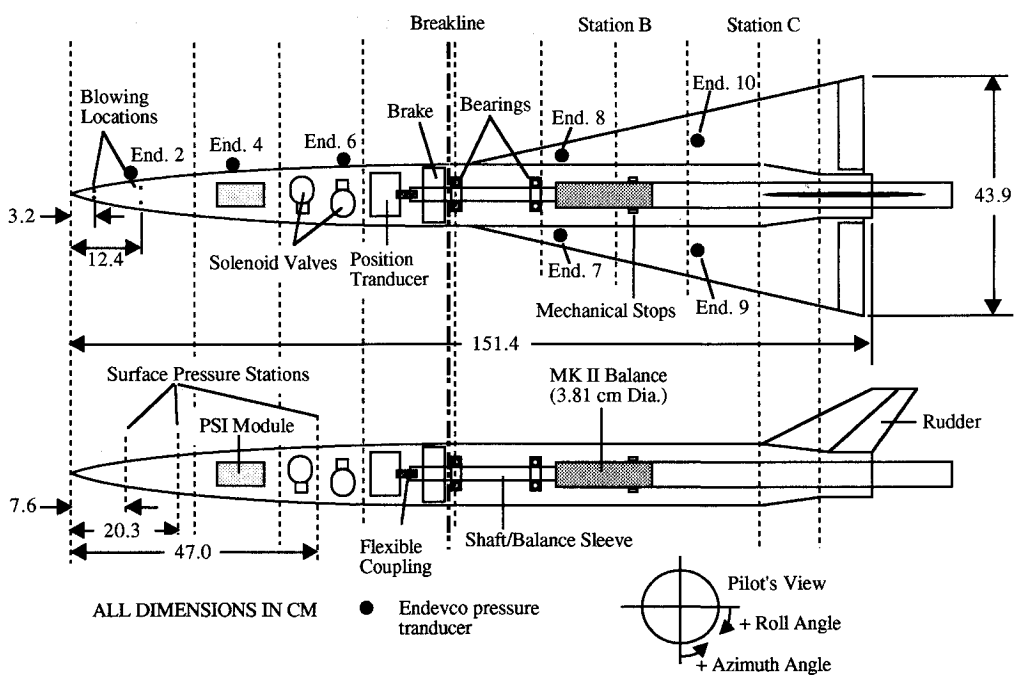

Fig. 1 Schematic of the wind-tunnel model. All dimensions are in centimeters.

zation that was recorded using both a 35-mm camera and a ¾-in. videotape recorder. The vortex flow was visualized using either regular floodlight or a laser sheet. Selected video recordings were digitized using a video digitizer, and the resulting images were enhanced and analyzed.

Most of the static and free-to-roll experiments were carried out at angles of attack from 0 to 30 deg. Additional water-tunnel tests at higher angles of attack were conducted for specific configurations.

III. Results

A. Static Behaviors

Water-tunnel tests were performed with the model statically fixed at different angles of attack. The forebody flow of the water-tunnel model becomes visibly asymmetric at α above about 25 deg. The forebody vortex on each side can be seen to interact directly with the corresponding wing vortex. This interaction causes a portion of the wing vortex near the trailing edge to lift away from the surface. The natural model asymmetry favors the right forebody vortex being farther from the surface than the left. This right vortex, high-forebody flow asymmetry increases progressively with the angle of attack. At α = 30 deg (Fig. 2), where the forebody flow is strongly asymmetric, vortex breakdown moves upstream of the trailing edge of the left wing, but not the right. Also, the left (low) can be seen to interact directly with the right wing vortex. Similar results were obtained for model configurations with tail B and no tail. The corresponding wind-tunnel tests show zero-sideslip yawing and rolling moments for α above about 15 deg.

The water-tunnel flow visualizations demonstrate the effect of blowing on the forebody vortex asymmetry over the static model. At α = 30 deg, two effects can be observed when blowing underneath the low (left) vortex. First, the natural right vortex high-forebody flow asymmetry is enhanced. Second, the aft portion of the left (low) forebody vortex is lifted farther from the wing surface by blowing. Eventually, the direct interaction between the left forebody vortex and the wing vortex is suppressed. When blowing underneath the high (right) vortex at increasing blowing rate, the natural forebody vortex-asymmetry is reduced and eventually reversed. Again, once the right forebody vortex moves sufficiently far from the wing surface, direct interactions between the forebody and the wing vortices are suppressed. Therefore, the forebody-wing vortex interaction on either side of the model can be suppressed by inducing with blowing a large forebody vortex asymmetry. The wing vortex breakdown asymmetry switches correspondingly when the orientation of the forebody vortex asymmetry is switched by blowing. This indicates that the asymmetry in wing vortex breakdown is dictated to a significant extent by the forebody vortex asymmetry. The yawing and rolling moments from the wind-tunnel tests generally confirm the predictions from the flow visualization results.

B. Free-to Roll Tests: Roll Angle History

For the water-tunnel experiment, tests were performed with the model mounted on the free-to-roll bracket to investigate the effect of releasing the constraint on the roll axis. Three model configurations were tested: 1) the model with no vertical tail (model O or NT), 2) with tail A (model A), and 3) with tail B (model B). A roll angle that results in a right-wing-down attitude is designated as positive, while an angle that results in a left-wing-down attitude is negative. Correspondingly, clockwise and counterclockwise rotations from a pilot's viewpoint are designated as positive and negative, respectively.

For the water-tunnel model O at α below 23 deg, the model will roll to a certain negative (left-wing-down) roll angle when released from rest. However, no wing rock was observed. Therefore, the natural flow asymmetry causes the model to roll to a negative roll position that is both statically and dynamically stable in roll. Above α = 23 deg, a limit cycle wing rock occurs with the amplitude increasing with the angle of attack. Beyond the angle-of-attack range where wing rock initially occurs, the model oscillates in a relatively regular frequency about a negative mean roll position. The time required to establish a limit-cycle wing-rock motion decreases with angle of attack. The roll angle history results of models A and B are qualitatively similar to those of model O.

The wind-tunnel tests were conducted with the tail-on and tail-off configurations. The angular displacement transducer was used to measure the roll angle of the wind-tunnel model during the wing rock motion. Data were acquired during 3 s at 200 samples/s, providing an accurate roll angle history. Data were also taken with an oscillograph recorder (OGR) for longer periods of time to investigate wing rock buildup and wing rock suppression by blowing.

The wing rock motion of the wind-tunnel model starts at α = 22 deg. For angles of attack below 22 deg, the model either rolls to a position that is statically and dynamically stable, or experiences irregular motions. The time required to establish a limit-cycle wing-rock motion decreases with angle of attack. The roll angle history results of the tail-off configuration are qualitatively similar to the tail-on results.

In both the wind- and water-tunnel tests, the reduced frequency generally increases with the angle of attack. The wind-tunnel results also indicate that the reduced frequency decreases with increasing freestream velocity, with the exception of α = 22 deg. The reduced frequency of wing rock is significantly higher in the water-tunnel tests. This is expected because of the large difference in inertial scaling of the models in water and in air.

C. Contributions of Model Components to Wing Rock

1. *Role of the Vertical Tail*

The peak-to-peak wing rock amplitudes for the three water-tunnel model configurations as a function of the angle of attack are shown in Fig. 3. As demonstrated in this figure,

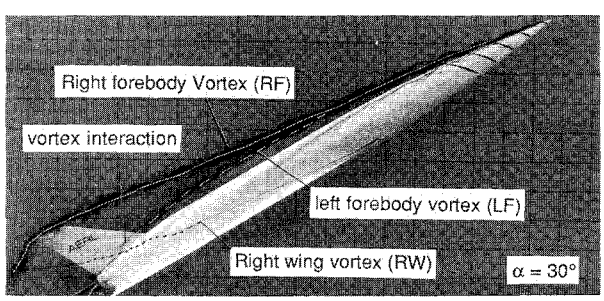

Fig. 2 Off-body flow visualization of the water tunnel model at α = 30 deg, static condition.

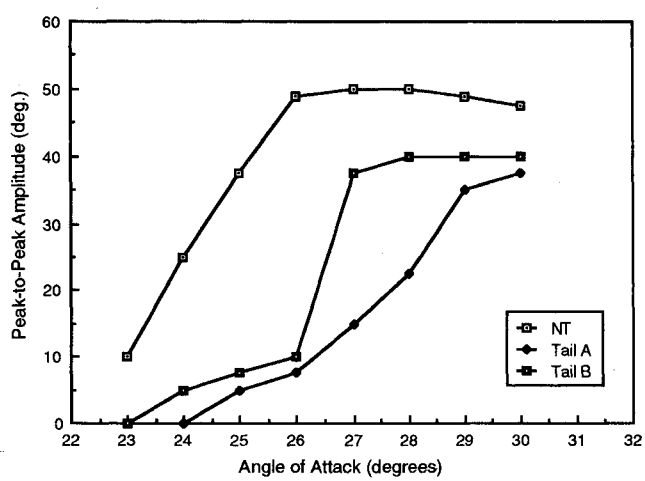

Fig. 3 Amplitude of the wing rock motion of the water-tunnel model.

the presence of a vertical tail delays the onset and reduces the amplitude of wing rock. One of the principle effects of the vertical tail in the water-tunnel tests is therefore to provide additional roll damping. The results, however, also show that a larger tail (tail B) can result in less overall roll damping than a smaller one (tail A). This suggests that the interaction between the tail surface and the flows off other parts of the model may be an important factor. Flow visualization results indicate that the main interaction is between the tail and the forebody vortices. Nevertheless, the results indicate that the net effect of a vertical tail is to increase roll damping in the water-tunnel experiments. This agrees with the experiment of Brandon and Nguyen,[3] where the removal of the vertical tail on a generic fighter configuration significantly increased the amplitude of wing rock.

Figure 4 shows the wing rock amplitudes for the wind-tunnel model configurations. The maximum peak-to-peak amplitude is smaller for the tail-off configuration than for the tail-on case. Thus, contrary to the water-tunnel results, the net effect of the tail of the wind-tunnel model is to decrease roll damping. This denotes further the potentially opposite roles of the vertical tail under different situations.

Balance-fixed normal and side forces were acquired in the wind-tunnel tests, and later reduced and converted to body-fixed coordinates by applying a transformation to account for the roll angle. Tares and balance interactions were not applied, and the actual magnitude of the coefficients could present a small error. The actual magnitude, however, is of secondary interest in this case; the behavior of the forces and their phase relationship with the motion is the information of primary interest.

Figure 5 shows the side force coefficients with and without tail during the wing rock motion at $\alpha = 28$ deg. The side force behavior for the tail-off case is as expected if there are no other major inputs than the body normal force component due to roll angle. The side force is zero (or near zero, due to time lag and/or the natural flow asymmetry) at $\phi = 0$ deg, and near maximum and minimum at the roll angle extremes. The side force for the tail-on configuration is significantly different from the tail-off case. One may assume that the differences between the results can be attributed mostly to the forebody vortices acting on the tail. Flow visualization in the water tunnel reveals that at any given time during the wing rock motion only one of the forebody vortices acts on the tail. A positive side force input from the interaction between the forebody vortex and the tail would therefore induce a positive rolling moment input. A comparison between the tail-on and tail-off side force results reveals that the rolling moment contribution from the tail can be propelling or restoring during the wing rock motion. Near the roll angle extremes, the tail-contributed rolling moment switches sign continuously, this is probably a result of the forebody vortex moving from one side of the vertical tail to the other. Apparently, the net effect on this model at the flow conditions tested is destabilizing. The tail also amplifies the effect of the natural flow asymmetry that results in different magnitudes of side force for positive and negative roll angles of the same magnitude (which is weakly evident with the tail-off).

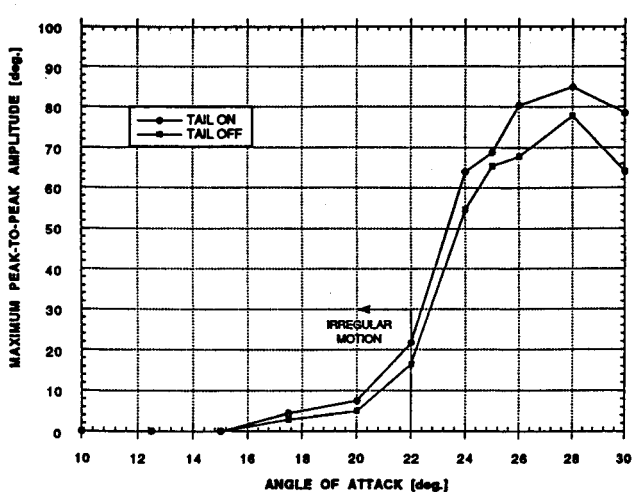

Fig. 4 Amplitude of the wing rock motion of the wind-tunnel model.

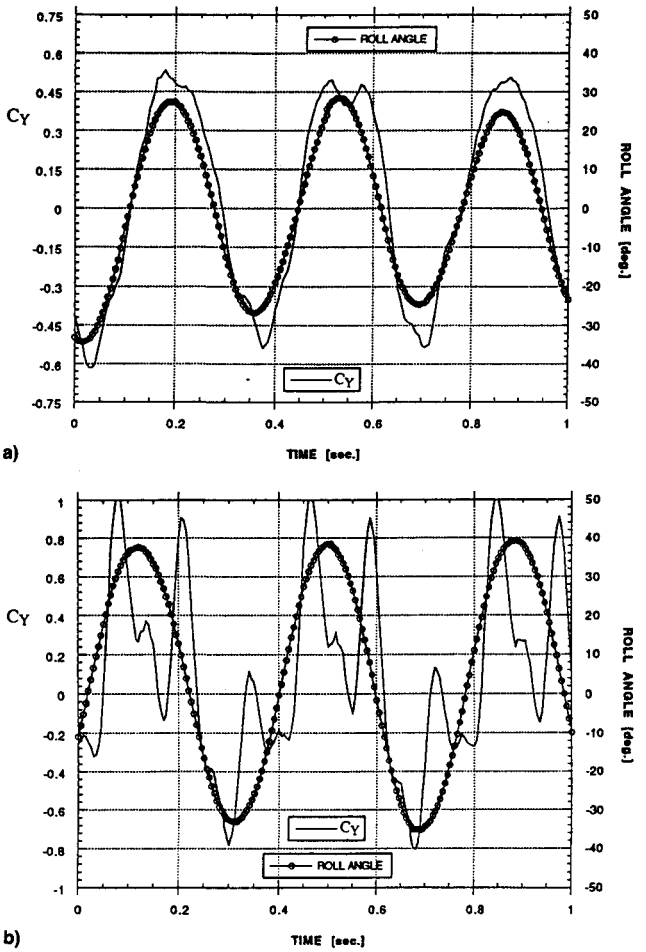

Fig. 5 Sideforce measurements during wing rock of the wind-tunnel model at $\alpha = 28$ deg: a) tail-off and b) tail-on.

Since wing rock occurs even in the absence of a vertical tail, the tail surface is not necessary for sustaining the wing rock motion of this model. Nevertheless, the presence of a vertical tail can increase or decrease the magnitude of wing rock. For instance, one of the main differences between the water-tunnel model and wind-tunnel model during wing rock is the much higher reduced frequency for the former. The convective time lag associated with the interaction between the forebody vortices and the tail should be much more pronounced in the water-tunnel tests. The phase between the rolling moment contribution from the tail and the body roll motion can therefore be significantly different between the water- and wind-tunnel experiments. Depending on the specific phase relationship, the rolling moment from the tail can be propelling or restoring.

2. *Roles of the Forebody and Wings*

Water-tunnel tests were performed with the forebody forward of the breakline (see Fig. 1) removed and the fuselage operating in a flow-through mode to study the role of the wings in wing rock. Flow visualization did not reveal any strong direct effects on the wing vortices due to the removal of the forebody. Obviously, the interaction between the forebody and wing vortices at moderate-to-high angles of at-

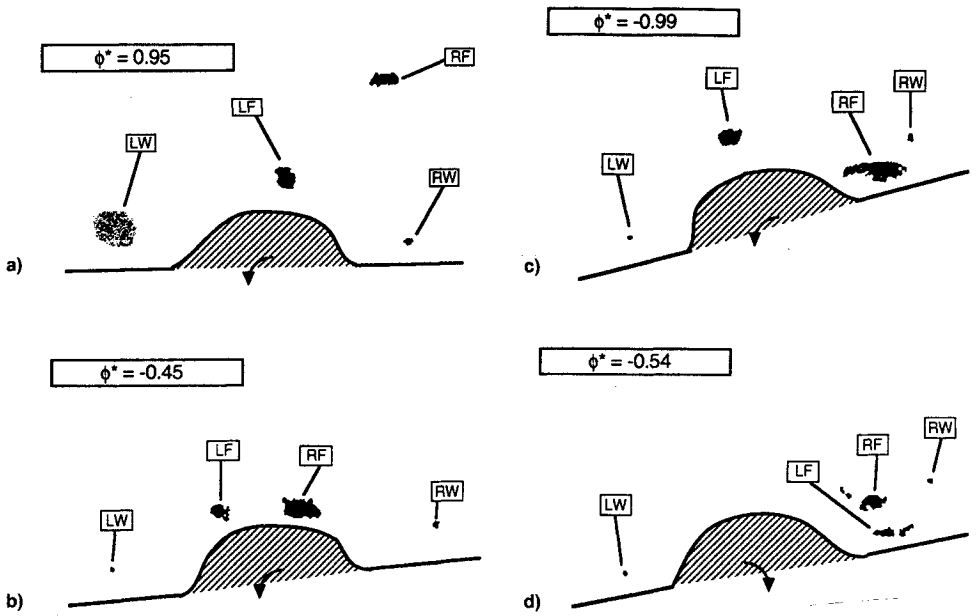

Fig. 6 Water-tunnel laser-sheet visualization of the vortices at station C during wing rock of the model at α = 29 deg.

tack is absent. At conditions where the forebody vortices would be strongly asymmetric, such as the case of α = 30 deg, the interaction between the vortices causes vortex breakdown to occur over only one of the wings as described earlier. Removal of the forebody, on the other hand, results in vortex breakdown over both wings. Thus, one effect of the interaction between the forebody and wing vortices is to delay vortex breakdown over one wing.

Without the forebody, no wing rock was observed over the range of angle of attack tested (up to 50 deg). Any roll motion induced by random disturbances was readily damped out. Thus, in the absence of the forebody, the wing flow alone is not capable of establishing a limit-cycle wing-rock motion. In comparison, a pure delta wing with the same sweep can be expected to wing rock for an angle-of-attack range from about 24 to 50 deg.

Since the forebody and fuselage are circular in cross section, the asymmetry in surface pressure cannot induce a roll moment about the roll axis that is centrally located about the fuselage. Therefore, except for possibly a small (damping) effect from the skin friction, the above results suggested that wing rock of this configuration was dictated by interactions between the forebody vortices and wing surfaces of the model. To understand the process more thoroughly, flow visualizations were used to study the vortex flow in detail.

The flow visualization results reveal that through the wing rock cycle, the forebody vortices lift off alternatively from the body surface. A significant convective time-lag was observed when the vortex first lifts off at the nose tip and propagates downstream while the model is in continuous motion. Strong interactions between the forebody and the wing vortices can also be observed, especially towards the trailing half of the wings. Due to the natural forebody flow asymmetry, the main interactions are concentrated over the right wing, with the rear portion of the wing vortex being lifted farther from the wing surface.

The flow visualization using a laser sheet was used to study in detail the interactions between the forebody and wing vortices at different streamwise locations. At station B (Fig. 1 for corresponding location on the wind-tunnel model), there is very little direct interaction between the forebody and wing vortices. The left and right forebody vortices lift alternatively from the surface during the wing rock motion. On the other hand, positions of the left and right wing vortices relative to the respective wings do not change significantly. There is an absence of the distinct vortex lift-off behavior commonly observed on highly swept, pure delta wings during wing rock.[2] These vortex flow behaviors persist until farther downstream, where the forebody vortex asymmetry develops to a sufficiently large degree for the forebody vortices to interact directly with the wing vortices. This will be illustrated by the results at station C (Fig. 1 for station position).

Figure 6 shows the laser sheet visualization results at model station C during one cycle of wing rock motion at α = 29 deg. Near the maximum positive roll angle (Fig. 6a), and contrary to what may be expected for pure delta wings, vortex breakdown propagates upstream of the left (leeward) wing trailing edge. The rolling moment in the counterclockwise direction is therefore enhanced. Apparently, this breakdown behavior is a result of the interaction between the forebody and wing vortices as discussed earlier. During this phase of the model motion, the right forebody vortex moves continuously towards the surface, and the vortex breakdown over the left (windward) wing moves downstream of the trailing edge. At $\phi^* = -0.45$ and rolling counterclockwise (Fig. 6b), the left forebody vortex moves to a position farther off the surface than the right. The model continues to roll in the counterclockwise direction and at $\phi^* \approx -0.99$ (Fig. 6c), the right forebody vortex begins to lift from the surface. The process continues with the left vortex moving towards the right wing. At $\phi^* \approx -0.54$ (Fig. 6d) and rolling clockwise, portions of both forebody vortices are residing over the right wing at station C. Correspondingly, the right wing vortex is lifted farther from the wing surface. A positive rolling moment is produced during this sequence of vortex interactions to eventually induce a positive (clockwise) rolling motion. Note that a clockwise rolling moment is generated when small portions of the forebody vortices are both residing over the right wing. Therefore, the rolling moment that may have been generated by these vortices acting on the right wing is apparently small compared with that generated by the wing vortices. As the positive roll motion progresses, the forebody vortices move to the left, while the right forebody vortex continues to lift from the surface at the same time.

Pressures were measured on the wings of the wind-tunnel model with the Endevco pressure transducers. Figure 7 presents the pressure on the wings at the aft pressure station during one cycle of motion at 28-deg angle of attack. The results reveal a more symmetric flow behavior during wing rock when compared with the flow visualization results of the water-tunnel model. The plot resembles the typical rolling moment behavior during the wing rock of pure delta wings,

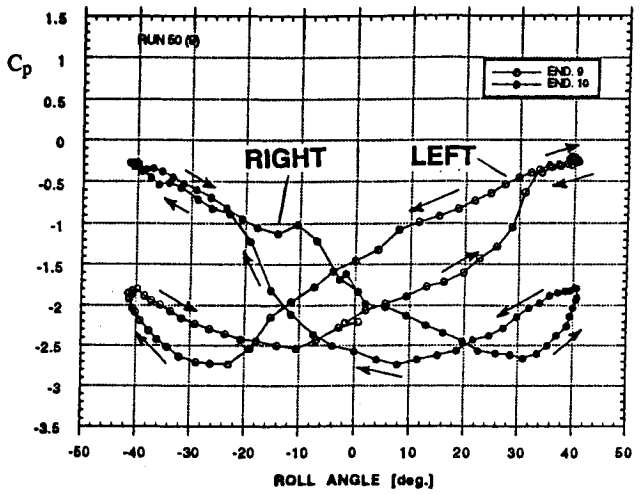

Fig. 7 Wing pressure distribution during wing rock motion of the wind-tunnel model at α = 28 deg—tail-on.

destabilizing at small roll angles and restoring at large roll angles.

Thus, the water-tunnel flow visualization and the wind-tunnel wing pressure results reveal that the wing vortices provide the necessary rolling moments for wing rock. However, the wing rock motion is controlled mainly by the behavior of the forebody vortices during the roll motion. The exact processes involved are undoubtedly dependent on the specific model and the flow conditions. Nevertheless, the controlling of the positions and breakdown of the wing vortices by the forebody vortices should be one of the primary mechanisms that sustain a wing rock motion.

The wing rock motion at initial sideslip conditions was investigated in the wind tunnel. Results of Nguyen et al.[16] show that a flat 80-deg delta wing does not exhibit wing rock at a mean sideslip angle of 10 deg. Contrary to the pure delta wing results, strong wing rock persists even at a mean sideslip of -10 deg. Although the amplitude is smaller than at zero sideslip condition, a significant decrease in the amplitude is seen only when the angle of attack is increased to 30 deg. This is another indication of the differences between the wing rock mechanism between slender delta wings and body-wing configurations. The interactions among vortices and aircraft components are major participants in the wing rock phenomenon observed in this type of configuration.

D. Control of Wing Rock by Forebody Blowing

One means of suppressing the wing rock motion is to directly control the forebody vortices that control the wing rock of this configuration. Two methods of control were investigated: 1) steady and 2) alternating jet blowing. Examples of the results will be discussed below.

1. Steady Blowing

The water-tunnel tests show that at low blowing rates, the wing rock amplitude is reduced. The effect can be achieved by blowing from either the left or right side, although the blowing rates required are different due to the natural flow asymmetry. Above a certain blowing rate that is dependent on the angle of attack and natural flow asymmetry, wing rock can be stopped entirely. Under this condition, the wing rock motion can be damped within about one cycle of motion by steady blowing on either side of the forebody. However, it is not possible to suppress wing rock while maintaining a zero-roll position. Results of all models are similar.

Blowing experiments were performed on the wind-tunnel model at α = 25 and 30 deg. Overall, the results are qualitatively similar to those of the water-tunnel tests. A strong asymmetric yawing moment was observed in the static tests at 30-deg angle of attack, signifying a right vortex, low-forebody flow pattern. At C_μ = 0.0028, blowing under the right (low) vortex suppresses wing rock entirely. The motion is stopped with the model presenting a right-wing-down attitude at a roll angle of approximately 10 deg. Blowing underneath the left (high) vortex at C_μ = 0.0028 reduces the amplitude, but does not eliminate wing rock completely. By increasing C_μ to 0.0037, blowing on either side can suppress wing rock entirely. Right and left blowing result in the model stopping at roll angles of 10 and -10 deg, respectively. Interestingly and contrary to what one may predict, the model stops at $\phi = -10$ deg instead of 10 deg when blowing on both sides at C_μ = 0.0037.

Water-tunnel flow visualization results such as Fig. 8 reveal that steady blowing on either side of the forebody suppresses wing rock by "locking" the forebody vortex asymmetry into a pattern that prevents interactions with the wing vortices. In addition to the nonzero roll angle, a large yawing moment can result from the highly asymmetric forebody vortex pattern. This is confirmed by the wind-tunnel force and moment measurements. These side effects probably make this means of control undesirable.

An attempt was made to eliminate the vortex asymmetry while simultaneously suppressing wing rock by blowing at different rates on both sides of the forebody of the water-tunnel model. In this water-tunnel experiment, blowing on one side was fixed initially at a rate that would suppress wing rock. After steady state was reached for the blowing condition, blowing on the other side was turned on. The model motion and vortex flow were observed and, at selected conditions, the roll angle history was determined. Examples of roll angle history of cases fixing the blowing rate on the left side and varying the blowing on the right are shown in Fig. 9.

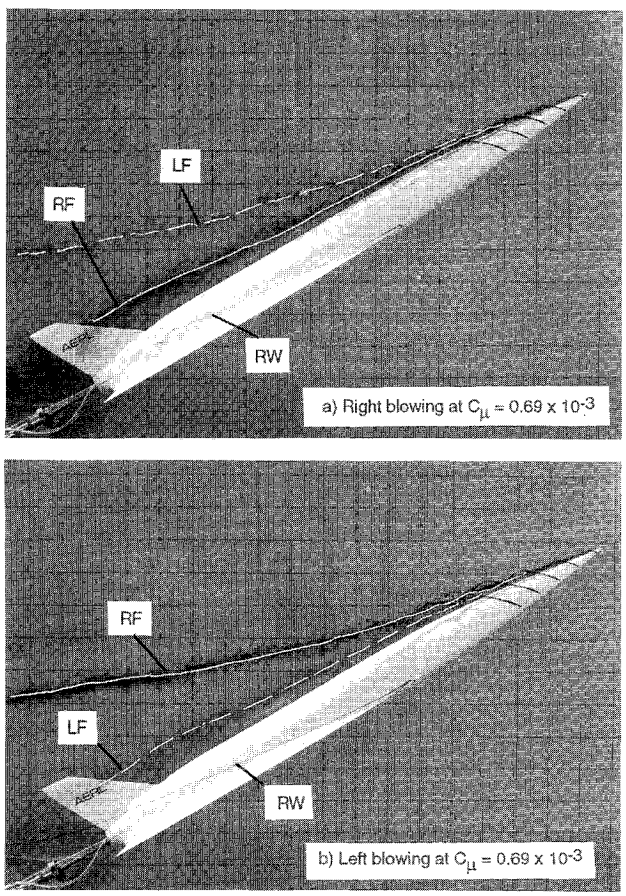

Fig. 8 Off-body flow visualization of the effect of forebody blowing on the model at α = 30 deg, free-to-roll condition.

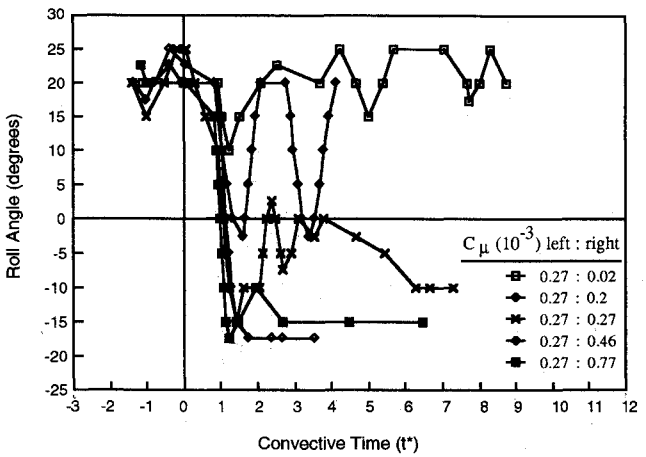

Fig. 9 Effect of simultaneous steady blowing on both sides of the water-tunnel model A at α = 29 deg.

In Fig. 9, the left blowing is fixed at $C_\mu = 0.27 \times 10^{-3}$, a rate that is just sufficient to suppress wing rock with left blowing alone. Increasing the right blowing from $C_\mu = 0$ to 0.02×10^{-3} causes the model to roll initially in the negative direction, but the effect diminishes and the steady-state model behavior is essentially the same as left blowing alone. Increasing the right blowing to $C_\mu = 0.2 \times 10^{-3}$ again causes the model to roll initially in the negative direction. However, a wing rock motion with a bias towards negative roll is eventually established. The peak-to-peak wing-rock amplitude is about 22 deg, compared with 35 deg for the no-blowing case (Fig. 3). At a right-blowing rate of $C_\mu = 0.27 \times 10^{-3}$, the model rolls initially to a negative angle of about 20 deg. Eventually, the model reaches a steady-state roll angle of -10 deg after a relatively long transient period. The behaviors at right blowing rates of $C_\mu = 0.46 \times 10^{-3}$ and 0.77×10^{-3} are essentially the same, except that the transient period decreases and the magnitude of the steady-state roll angle increases with increased blowing.

The simultaneous steady blowing results show that the configuration becomes unstable in roll and starts to rock when the blowing rates on the two sides are adjusted to maintain a near symmetric forebody vortex pattern. That is, without creating a sufficiently large forebody vortex asymmetry, wing rock will persist. One of the reasons for this behavior is revealed by the flow visualization of the static model. When the forebody flow is forced by blowing to become almost symmetric at high angles of attack, a strong interaction between the forebody and wing vortices occurs. This vortex interaction produces a dynamically unstable situation that results in wing rock. Therefore, using steady blowing to suppress wing rock, but without creating a large forebody vortex asymmetry, may not be feasible for this configuration at moderate-to-high angles of attack.

2. Alternating Pulsed Blowing

Since steady blowing can be used to achieve wing rock suppression seemingly only at the expense of potentially undesirable aerodynamic side effects, another scheme of control was attempted. In this scheme, blowing was pulsed alternatively between the left and right nozzles at a high frequency. The idea is to create a forebody vortex pattern that is symmetric on a time-averaged basis while simultaneously suppressing wing rock.

Pulsed blowing was evaluated in the wind tunnel at α = 30 deg and $C_\mu = 0.0028$ at different frequencies. At low frequencies, the blowing is not effective in suppressing wing rock. When pulsing at frequencies close to the natural wing rock frequency, the wing rock motion can be either enhanced or damped, depending on the phase relationship between the motion and the blowing. Blowing at frequencies two to three times (6–9 Hz) the wing rock frequency reduced the wing rock amplitude substantially. Blowing at frequencies higher than 9 Hz was less effective during the wind tunnel tests; this was likely due to the failure of the blowing pressure at the nozzle to reach the required level for effectiveness.

Figure 10 presents OGR data of the effect of pulsed blowing at 6 Hz. The natural wing rock is nearly eliminated. The model, however, oscillates at approximately the pulsed frequency (twice the natural wing rock frequency) at a low amplitude. This indicates that the model is responding to the unsteady flowfield induced by the pulsed blowing—a phenomenon that may be eliminated at higher pulsing frequencies due to natural damping. The yawing moment for the model in a static position is shown in Fig. 11. For the range of pulsing frequency where wing rock suppression is effective, the yawing moment is almost zero, indicating that the forebody flow is symmetric on a time-averaged basis. Therefore, the major advantages of pulsed blowing appear to be its ability to suppress wing rock without creating a large forebody asymmetry. In addition, for a given blowing coefficient, the required total mass flow for a given period is less than for continuous blowing.

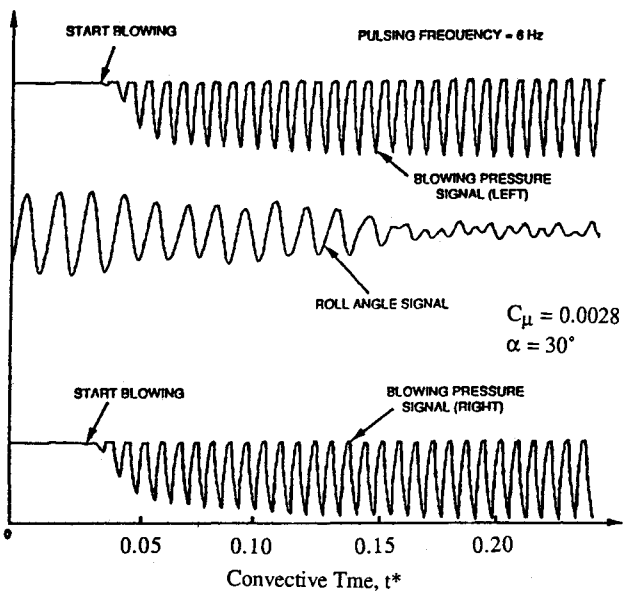

Fig. 10 Effect of alternating pulsed blowing on the wind-tunnel model at α = 30 deg (tail-on and pulsed blowing at two times the natural wing rock frequency).

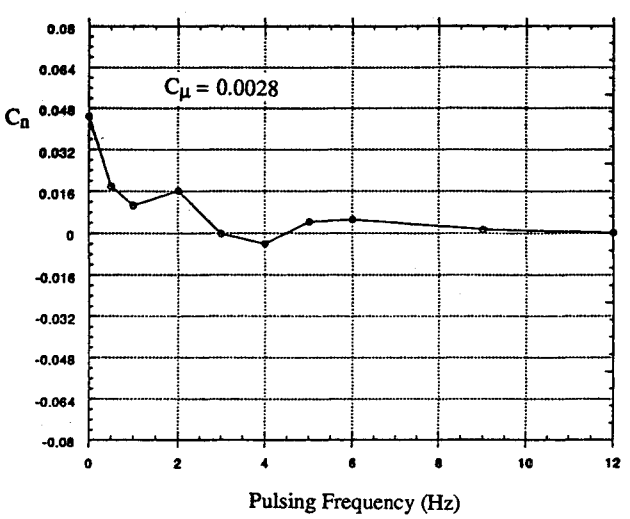

Fig. 11 Influence of pulsing frequency on the sideforce coefficient of the wind-tunnel model at α = 30 deg. Natural wing rock frequency = 3.0 Hz.

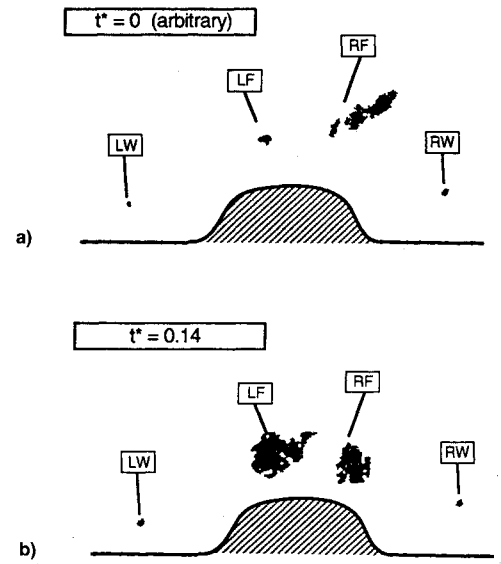

Fig. 12 Water-tunnel laser-sheet visualization of the effect of pulsed blowing on the vortices at station C of the model at $\alpha = 29$ deg, free-to-roll condition.

In general, the water-tunnel results agree with these wind-tunnel results. At slow alternating rates, the blowing does not have significant effects on wing rock. The wing rock amplitude begins to decrease when the rate is increased. The trend continues, and at sufficiently high alternating rates, wing rock is completely suppressed. In flow visualizations the vortices show a wavy pattern, likely due to the convective time lag associated with pulsed blowing on both sides. Most importantly, as opposed to steady blowing at the same peak rates either individually or simultaneously on the left and right sides, a zero-roll position is maintained, while at the same time wing rock is suppressed. Results of laser sheet visualization at station C of model A at $\alpha = 29$ deg are shown in Fig. 12 for the case where the pulsed frequency is five times the wing rock frequency. The forebody vortices can be seen to oscillate between two asymmetric patterns with smaller degrees of asymmetry than in the case without blowing. The forebody vortex asymmetry never develops to a sufficiently large degree to result in strong interactions with the wing vortices. Therefore, the mechanism responsible for the wing rock of this configuration is suppressed.

IV. Conclusions

The wing rock characteristics of a highly slender configuration were investigated in a water tunnel and a wind tunnel. Different means of suppressing wing rock by controlling the forebody vortices were also explored. Several conclusions can be made.

1) Wing rock for the highly slender configuration tested is caused by the forebody vortices interacting with the wing flow. While the wing vortices seem to provide most of the rolling moments, the wing rock motion is controlled by the forebody vortices.

2) The presence of a fuselage between the left and right wing vortices prevents the types of wing rock and vortex motions observed on pure delta wings with the same sweep.

3) Steady blowing can suppress wing rock of this configuration, but only at the expense of the creation of significant vortex asymmetries.

4) Alternating pulsed blowing on the left and right sides of the forebody can potentially be an effective means of suppressing wing rock and simultaneously eliminating large asymmetric moments at high angles of attack.

The exact forms of interactions between the forebody flow and the other components of a configuration are no doubt dependent on the specific configuration and flow conditions. Nevertheless, it is believed that the concept of suppressing wing rock by controlling the forebody vortex flow should be generally applicable for situations where the primary controlling mechanism of wing rock is the forebody vortices.

Acknowledgments

Support for this work is provided by NASA Ames Research Center under Contract NAS2-12989. The technical monitor is Larry Meyn.

References

[1]Ericsson, L. E., "The Various Sources of Wing Rock," *Journal of Aircraft*, Vol. 27, No. 6, 1990, pp. 488–494.

[2]Ng, T. T., Malcolm, G. N., and Lewis, L. C., "Flow Visualization Study of Delta Wings in Wing-Rock Motion," AIAA Paper 89-2187, July–Aug. 1989.

[3]Brandon, J. M., and Nguyen, L. T., "Experimental Study of Effects of Forebody Geometry on High Angle of Attack Static and Dynamic Stability," AIAA Paper 86-0331, Jan. 1986.

[4]Brandon, J. M., Murri, D. G., and Nguyen, L. T., "Experimental Effects of Forebody Geometry on High Angle of Attack Static and Dynamic Stability and Control," 15th Congress of the International Council of the Aeronautical Sciences, London, Sept. 1986.

[5]Nguyen, L. T., Gilbert, W. P., Gera, J., Iliff, K. W., and Enovoldson, E. K., "Application of High-α Control System Concepts to a Variable Sweep Fighter Airplane," AIAA Flight Mechanics Conf., Danvers, MA, Aug. 1980.

[6]Ross, A. J., "Lateral Stability at High Angle of Attack, Particularly Wing Rock," AGARD CP-260, May 1979.

[7]Fratello, D. J., Croom, M. A., Nguyen, L. T., and Domack, C. S., "Use of the Updated NASA Langley Radio-Controlled Drop-Model Technique for High-Alpha Studies of the X-29A Configuration," AIAA Paper 87-2559, Aug. 1987.

[8]Murri, D. G., and Rao, D. M., "Exploratory Studies of Actuated Forebody Strakes for Yaw Control at High Angles of Attack," AIAA Paper 87-2557-CP, Aug. 1987.

[9]Malcolm, G. N., Ng, T. T., Lewis, L. C., and Murri, D. G., "Development of Non-Conventional Control Methods for High Angle of Attack Flight Using Vortex Manipulation," AIAA Paper 89-2192, July–Aug. 1989.

[10]Zilliac, G., Degani, D., and Tobak, M., "Asymmetric Vortices on a Slender Body of Revolution," AIAA Paper 90-0388, Jan. 1990.

[11]Moskovitz, C., Hall, R., and DeJarnette, F., "Experimental Investigation of a New Device to Control the Asymmetric Flowfield on Forebodies at Large Angles of Attack," AIAA Paper 90-0068, Jan. 1990.

[12]Ng, T. T., and Malcolm, G. N., "Aerodynamic Control Using Forebody Strakes," AIAA Paper 91-0618, Jan. 1991.

[13]Tavella, D. A., Schiff, L. B., and Cummings, R. M., "Pneumatic Vortical Flow Control at High Angles of Attack," AIAA Paper 90-0098, Jan. 1990.

[14]Rosen, B., and Davis, W., "Numerical Study of Asymmetric Air Injection to Control High Angle-of-Attack Forebody Vortices on the X-29 Aircraft," AIAA Paper 90-3004, Aug. 1990.

[15]Ng, T. T., and Malcolm, G. N., "Aerodynamic Control Using Forebody Blowing and Suction," AIAA Paper 91-0619, Jan. 1991.

[16]Nguyen, L. T., Yip, L., and Chambers, J. R., "Self-Induced Wing Rock of Slender Delta Wings," AIAA Paper 81-1883, Aug. 1981.